Chaos
An Interdisciplinary Journal of Nonlinear Science

RESEARCH ARTICLE | AUGUST 03 2023

Robustness of directed higher-order networks

Dandan Zhao; Xianwen Ling; Xiongtao Zhang; Hao Peng ; Ming Zhong ; Cheng Qian ; Wei Wang

Chaos 33, 083106 (2023)
https://doi.org/10.1063/5.0159943

Chaos ARTICLE pubs.aip.org/aip/cha

Robustness of directed higher-order networks

Cite as: Chaos 33, 083106 (2023); doi: 10.1063/5.0159943
Submitted: 29 May 2023 · Accepted: 11 July 2023 ·
Published Online: 3 August 2023

Dandan Zhao,[1] Xianwen Ling,[1] Xiongtao Zhang,[2] Hao Peng,[1,3] Ming Zhong,[1] Cheng Qian,[1] and Wei Wang[4,a)]

AFFILIATIONS

[1]School of Computer Science and Technology, Zhejiang Normal University, Jinhua 321004, Zhejiang, China
[2]School of Information Engineering, Hu zhou University, Huzhou 313000, China
[3]Key Laboratory of Intelligent Education Technology and Application of Zhejiang Province, Zhejiang Normal University, Jinhua 321004, China
[4]School of Public Health, Chongqing Medical University, Chongqing 400016, China

[a)]**Author to whom correspondence should be addressed:** wwzqbx@hotmail.com

ABSTRACT

In complex systems, from human social networks to biological networks, pairwise interactions are insufficient to express the directed interactions in higher-order networks since the internal function is not only contained in directed pairwise interactions but rather in directed higher-order interactions. Therefore, researchers adopted directed higher-order networks to encode multinode interactions explicitly and revealed that higher-order interactions induced rich critical phenomena. However, the robustness of the directed higher-order networks has yet to receive much attention. Here, we propose a theoretical percolation model to analyze the robustness of directed higher-order networks. We study the size of the giant connected components and the percolation threshold of our proposed model by the theory and Monte-Carlo simulations on artificial networks and real-world networks. We find that the percolation threshold is affected by the inherent properties of higher-order networks, including the heterogeneity of the hyperdegree distribution and the hyperedge cardinality, which represents the number of nodes in the hyperedge. Increasing the hyperdegree distribution of heterogeneity or the hyperedge cardinality distribution of heterogeneity in higher-order networks will make the network more vulnerable, weakening the higher-order network's robustness. In other words, adding higher-order directed edges enhances the robustness of the systems. Our proposed theory can reasonably predict the simulations for percolation on artificial and real-world directed higher-order networks.

In a real network, explicitly encoded multi-node interactions can be used to portray higher-order networks and reveal the rich criticality phenomena induced by higher-order interactions. Therefore, researchers have proposed using higher-order networks to measure the robustness of complex systems, and studying the influence of directivity in higher-order networks is a significant problem. In this paper, we propose a theoretical framework to analyze higher-order directed networks and measure the robustness of different networks by analyzing the percolation process through hyperdegree distribution and hyperedge cardinality. We also verify the influence of higher-order directed edges on real network environments. These findings provide valuable insights into how the underlying structure of directed higher-order networks shapes network resilience, contributing to a deeper comprehension of this relationship.

I. INTRODUCTION

With the availability of real data, researchers have effectively portrayed the relationships in real-world networks through network descriptions.[1] In general, the edges of the network are mapped as interactions between various elements, and edges connect two vertices by modeling the nodes in the network as components of a complex system. It can be divided into an undirected network and a directed network according to whether the connection relation is directed. Undirected networks can portray Internet networks,[2] and directed networks can portray social networks,[3,4] biological networks,[5,6] and email networks.[7] However, in the real world, almost all networks can be subject to targeted attacks or random failures.[8–10] For example, in May 2017, the WannaCry ransomware virus broke out worldwide through the MS17-010 vulnerability for financial purposes, forming a worm storm that affected the world.[11]

In September 2019, bushfires in northern New South Wales, Australia, broke out suddenly and lasted for more than four months, destroying 10.7 million hectares of forest and bush, killing about 1 billion animals, causing irreversible damage to the ecosystem and a $ 5 billion in economic losses.[12] In March 2022, a massive power outage occurred in Taiwan, China. The semiconductor, optoelectronics, and Apple supply chain systems were hit hard, and the loss of manufacturers amounted to NT $6 billion.[13] In order to better protect the actual system, how to measure the robustness of the network is worth our attention.

As a vital method for studying complicated real-world systems, the percolation theory can be utilized to investigate network connectivity and the robustness of directed networks.[14,15] For the bond (site) percolation, each edge (node) is occupied with probability p. With the increase of the occupation probability p, the network's giant strongly connected component (GSCC) gradually increases. When the GSCC changes from zero to non-zero, the occupation probability p_c is called the percolation threshold. Callaway *et al.*[16] studied site percolation and bond percolation through Erdös–Rényi (ER) network and found that the percolation threshold is inversely proportional to the average degree of the network. Given the directivity of edges, Boguñá and Serrano[17] proposed a general theory to study different strongly connected components of randomly directed networks and found that bidirectional edges act as a catalyst in directed random networks in the process of percolation. Unlike undirected networks, in directed scale-free networks, the percolation properties can be captured by the in- and out-degree distribution, Schwartz *et al.*[18] found that the critical index of percolation in scale-free networks strongly depends on the presence of correlation and the index of the degree distribution.

However, in biological networks, ecology communities, and social networks, there is abundant evidence that pairwise interactions are insufficient to portray the real world.[19–21] Higher-order interactions in the real world occur not just between nodes but between three or more nodes.[22] Dynamics on higher-order networks have attracted much attention in the field of network science, including epidemic spreading,[23,24] synchronization,[25] and game.[26] Unlike traditional research focused on pairwise temporal effects on the single spreading dynamics, Nie *et al.*[27] proposed a coevolutionary epidemic spreading model over time higher-order social networks considering interactions and found that networks temporarily attenuate the effect of initial infection outbreak density thresholds. Alvarez-Rodriguez *et al.*[28] proposed a general implementation for collective games in which higher-order interactions are encoded on hypergraphs and found that additional game characteristics will facilitate the emergence of cooperation. Directed higher-order networks play an essential role in the application of higher-order dynamics. For instance, neurons are the vertices in the Caenorhabditis elegans neuronal network. These one or more synapses form the hyperedges of a network of neurons to build the higher-order network.[29] However, synapses are connected by a signal flow with direction, in order to analyze the directed interactions in neural networks more effectively, researchers express the higher-order interactions through directed higher-order networks.[30] Tang *et al.*[31] showed that higher-order interactions lead to topological synchronization phenomena beyond pairwise interactions. The structural symmetry can be preserved in the optimally synchronizable directed higher-order networks. It shows that the directed higher-order network plays an indispensable role in the field of higher-order network dynamics.

Although many efforts have been devoted to the dynamics of directed higher-order networks, the percolation of directed higher-order networks has not been studied until now. In this paper, we study the problem of measuring robustness on higher-order networks using the percolation theory. We generate a directed higher-order network of a specific scale by giving the hyperdegree k and the hyperedge cardinality m. The percolation threshold and the size of giant connected components (GCCs) are derived by using the generation function and self-consistent equation. In short, the main contribution of this paper is as follows.

- Proposing a directed higher-order network theoretical framework to study the robustness of higher-order networks. Mathematical formulas deduce the percolation threshold and the size of different GCCs. The results of simulations and theoretical results correspond to the artificial network we constructed.
- Revealing the effects of hyperdegree and hyperedge cardinality distribution heterogeneity on the higher-order network. The directed edges of the network are accompanied by a decrease in hyperdegree and hyperedge cardinality, the percolation threshold also decreases gradually. We conclude that the increase of higher-order directed edges enhances the system's robustness. In addition, finite scale effects positively affect the percolation process in heterogeneous directed higher-order networks.
- Our theory is validated on both artificial and real-world networks. We construct real-world networks and convert them into factor graphs to simulate the percolation process in real-world directed higher-order networks.

The rest of this article is structured as follows. In Sec. II, we reviewed the state of the art on percolation in higher-order networks. Section III describes the theoretical model in detail. After our derivation, Sec. IV introduces the simulation results of the artificially generated network and the real-world network. Finally, in Sec. V, the thesis is summarized, and future work has prospected.

II. RELATED WORKS

We mainly discuss percolation on two kinds of networks: directed pairwise networks and higher-order networks.

A. Percolation on directed networks

Generally, regardless of bidirectional links, each node in a directed simple pairwise network has two degrees, in- and out-degrees.[32] Therefore, the degree distribution of a directed network is a joint degree distribution $P(k_i, k_o)$ based on in- and out-degrees. $\Phi(x,y) = \sum_{k_i\,k_o}^{\infty} P\left(k_i, k_o\right) x^{k_i} y^{k_o}$, where k_i and k_o represents the in- and out-degree of the network, x and y denote any variable. As an essential method to study complex systems, percolation plays an indispensable role in analyzing the characteristics and structure of directed networks.[33–35] In studying the percolation of undirected networks, we usually discuss the size of GCCs, but the percolation of directed networks should consider more components. In this paper, we mainly consider three components:

- Giant Strongly Connected Component (GSCC): the strongly connected component in a directed network, where a vertex in GSCC can reach any other vertex in GSCC.
- Giant In-component (GIN): the nodes of GSCC plus the nodes leading to GSCC.
- Giant Out-component (GOUT): the nodes of GSCC plus the nodes leading from GSCC.

In the study of percolation on directed simple pairwise networks, Boguñá and Serrano[17] studied a general percolation theory for random directed networks with any two-point correlations and bidirectional edges in indicated random networks, opening new perspectives. Dorogovtsev *et al.*[36] calculated the GSCC of the directed network defined by Boguñá. Based on the GSCC of the general definition of the directed network, they found that the size of the GCC is closely related to the product of the in- and out-degree distribution and explained that the GSCC suffers small losses under random attacks. Serrano and De Los Rios[37] reanalyzed the traditional node percolation map of directed networks by organizing an edge into five branches during the process of edge percolation. It is divided into the edge in component, the in-the interface, the edge strongly connected component, the out interface, and the edge out component, and the final percolation simulation results are completely consistent with the theory. van der Hoorn and Litvak[38] analysis of degree dependence in complex networks and its impact on network processes requires null models, that is, models that generate uncorrelated directed scale-free networks. However, due to finite-size effects, the majority of models have demonstrated negative structural dependence. Using a rank-based correlation measure, we examine the behavior of these structures' negative degree dependence in a configuration model with directed erasure.

The above description introduces some of the work and problems encountered in the research of directed networks. Based on the previous theoretical knowledge of directed networks, we study some necessary properties in directed higher-order networks, including the GCCs and percolation threshold. In the process of studying directed scale-free networks, our model also exhibits some deviations due to finite-size effects, which will be discussed in Sec. IV.

B. Percolation on higher-order networks

In mathematical theory, an undirected higher-order network $H(V, E)$ is defined by a set of nodes, $V = \{v_1, v_2, \ldots, v_n\}$, and a set of m hyperedges $E = \{e_1, e_2, \ldots, e_m\}$, such that for all $\alpha = 1, \ldots, m$: $e_\alpha \subset V$.[39,40] If the number of hyperedges of a higher-order network is 2, then a higher-order network is equivalent to a simple pairwise network. That is, when the hyperedge cardinality of a higher-order network $m = 2$, a higher-order network is equivalent to a normal network. In a social higher-order network, where nodes represent users and hyperedges represent relationships between users (such as friendships), nodes: $\{A, B, C, D, E\}$, hyperedges: {{A, B}, {A, C, D}, {B, C}, {C, D, E}}, the hyperdegree of node A is 2, because of associated with it have $\{A, B\}$ and $\{A, C, D\}$. The hyperedge $\{A, B\}$ has A hyperedge cardinality of 2 because it connects nodes A and B, a total of 2 nodes. The hyperdegree is concerned with the number of connections between the node and the hyperedge, while the hyperedge cardinality is concerned with the number of nodes connected to the hyperedge. The analysis of social higher-order networks can help us to deeply understand the complex relationship between users, reveal the underlying structure and law of the network, and thus provide valuable insights for the management, optimization, and development of social networks.

In the paper of Sun and Bianconi,[41] a random higher-order network is defined as $\mathscr{H}(V, H)$, where V is a set of n distinct vertices and H is a set of hyperedges represented by m sizes of different hyperedge cardinalities. The number of hyperedges on a node is called the hyperdegree. For the convenience of calculation, it is necessary to transform the higher-order network into a factor graph. Factor graphs are associated with higher-order networks through simple mappings. The node set V and the node set H of the factor graph map to the node set V and the hyperedge set H of the higher-order network. The hyperdegree distribution $P(k)$ and the hyperedge cardinality distribution $P(m)$ correspond to the degree distribution of nodes and factor nodes in the factor graph, respectively, where the hyperdegree is represented by k and the cardinality size of the hyperedge is represented by m.

Percolation in undirected higher-order networks has attracted many researchers' interest. Peng *et al.*[42] describe the higher-order networks percolation under the network's target, through the theoretical framework to analyze random higher-order network robustness, and found the target attack easier than random attack to break down the higher-order network in addition to attacking the higher-order network nodes. Peng *et al.*[43] studied by attacking hyperedges to disrupt the higher-order network. When a high probability of removing hyperedges is found, the network becomes more and more fragile. In addition, Zhao *et al.*[44,45] used simplicial complexes to study the robustness of higher-order networks and found that double-phase transitions occur when the number of triangles exceeds a certain number. To better characterize the connectivity of higher-order networks, Kim and Goh[46] found the influence of higher-order components in the higher-order network. By introducing the concept of subgroups of nodes, confirmation of the existence of higher-order components will significantly impact contagion dynamics.

III. MODEL

Before introducing the directed higher-order network model, let us introduce the directed 2-hyperlink. As shown in Fig. 1(a), only the network with first-order interaction is studied in the directed pairwise networks. In the directed higher-order networks, we consider the directed 2-hyperlink interactions, describing pairwise interactions between elements of a complex system.[47] A directed 2-hyperlink is defined as the direction in which each permutation of the three nodes leads to a different 2-hyperlinks.[48] According to the directivity of edges, there are eight types of the directed 2-hyperlink in Fig. 1(a), and only 2 are shown here for simplicity. Our model needs to use this idea to reflect higher-order interactions in higher-order networks.

Without losing generality, we define a directed higher-order network through mathematical language. In Alain Bretto's higher-order networks review,[39] a directed higher-order network is defined as an ordered pair: $\vec{H} = \left(V; \vec{E} = \left(\{\overrightarrow{e_i} \; : i \in I\right)\right.$, where V is a finite set of vertices and $\vec{E}$ is a set of hyperedge with finite index set I. Each hyperedge $\overrightarrow{e_i}$ is an ordered pair. Similar to the definition of a higher-order network given in Sec. II B, in a directed higher-order

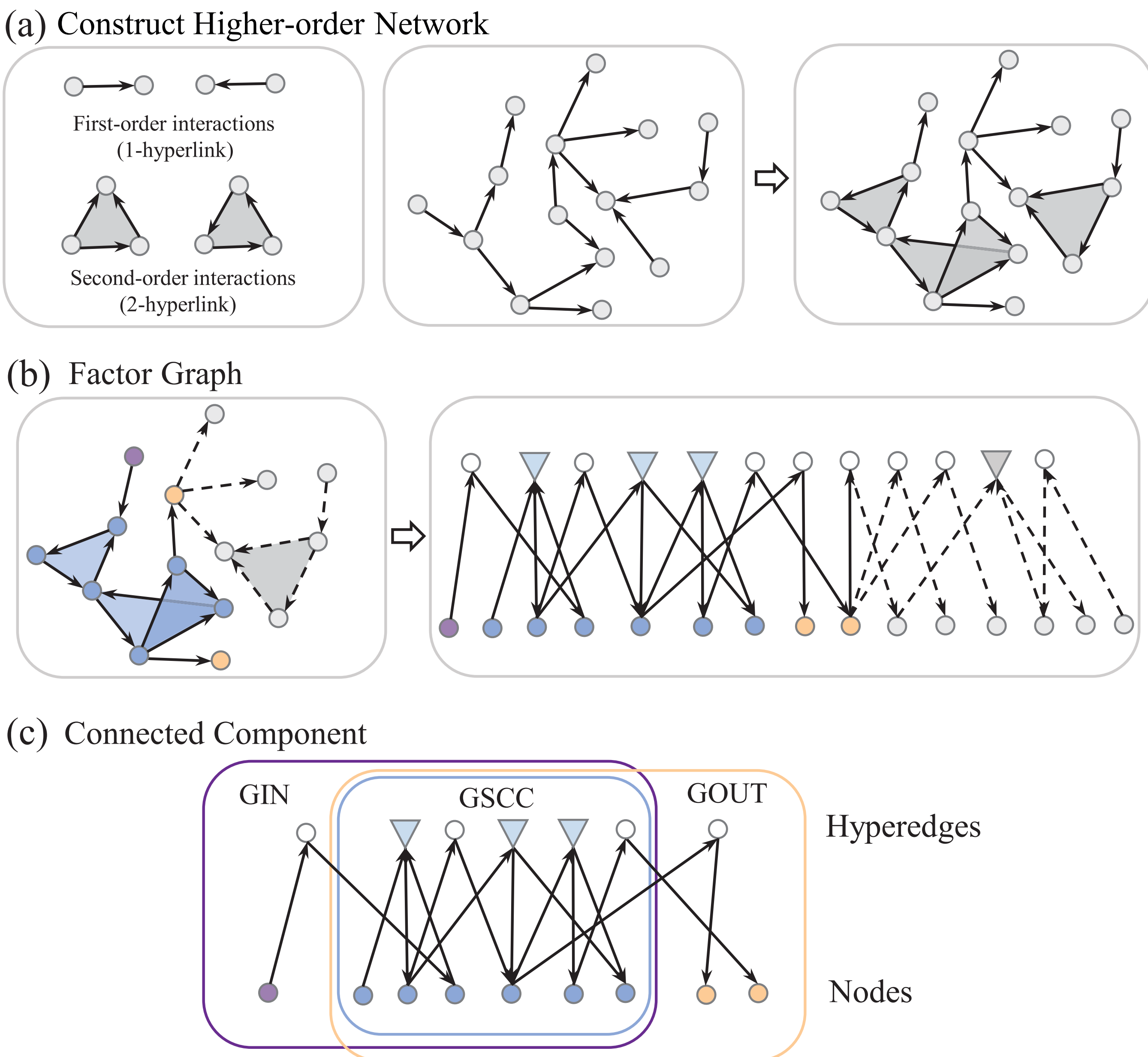

FIG. 1. Schematic on constructing the directed higher-order network, which is converted into a factor graph, and the size of each GCC of the network is obtained by percolating the factor graph. (a) Different order hyperlink and method of constructing directed higher-order model. First, the directed network is generated according to the generated degree distribution sequence, and then the directed triangle is randomly generated to construct the directed higher-order network. (b) The constructed higher-order network is converted into a factor graph. Solid lines connect the connected nodes. The upper layer represents the factor nodes and the hyperedges in the higher-order network, and the lower layer represents the vertices. The vertices are connected through directed interaction. (c) The light blue node set is GSCC, the GSCC node set and a purple node make up GIN, and the GSCC node set and two orange-gray nodes make up GOUT. The white nodes and triangles represent the hyperedges, and the columns below are the different nodes that correspond to the nodes in the higher-order network.

network, hyperedges represent the directed interaction of two vertices with directions. According to the definition of the directed higher-order network $G_{DH}(V, U, E)$, which is essentially a bipartite graph, after all, V is the set of nodes, U represents a set of factor nodes, E of the edges between the nodes and the factor nodes, and each interaction connects a node one-way to a factor node. The factor graph is related to the directed higher-order network by simply mapping. In the directed higher-order network, we introduce the concepts of k_i and k_o to represent the size of the in- and out-degree of the higher-order network, referred to as the hyperdegree, which means the number of nodes connected to factor nodes. The number of factor nodes connected to nodes is represented by m_i and m_o, referred to as hyperedge cardinality.

The following is our theoretical derivation from the generating function. The definition of the generating function of the in- and out-hyperdegrees distribution of the initial network node is as follows:[49]

$$G_0(x,y) = \sum_{k_i k_o} P(k_i,k_o) x^{k_i} y^{k_o}, \tag{1}$$

where $P(k_i, k_o)$ is the joint degree distribution of a directed higher-order network and x and y denote any variable. Since the sum of the in- and out-hyperdegrees is zero, $P(k_i, k_o)$ must satisfy the constraint

$$\sum_{k_i k_o} P(k_i,k_o)(k_i - k_o) = 0. \tag{2}$$

With G_0, we can define the generating functions G_0^i, which denotes the number of outward edges that leave a randomly chosen vertex the number of vertices leaving by following a randomly chosen edge, and G_1^i, which denotes the number leaving the vertex reached by following a randomly chosen edge,[50]

$$G_0^i(y) = G_0(1,y), \tag{3}$$

$$G_1^i(y) = \frac{1}{k_i} \frac{\partial G_0(x,y)}{\partial x}\bigg|_{x=1}. \tag{4}$$

Similarly, define the generating functions G_0^o and G_1^o for the number arriving at such a vertex,

$$G_0^o(x) = G_0(x,1), \tag{5}$$

$$G_1^o(x) = \frac{1}{k_o} \frac{\partial G_0(x,y)}{\partial y}\bigg|_{y=1}. \tag{6}$$

Average hyperdegree of a directed higher-order network,

$$\langle k \rangle = \sum_{k_i} P(k_i,k_o) k_i = \sum_{k_o} P(k_i,k_o) k_o. \tag{7}$$

Based on the definition of hyperedges, the generating function definition of the cardinality distribution of the in- and out-hyperedges of the initial network node is as follows:

$$\hat{G}_0(x,y) = \sum_{m_i m_o} \hat{P}(m_i,m_o) x^{m_i} y^{m_o}. \tag{8}$$

With $\hat{G}_0$, we can define the generating functions $\widehat{G}_0^i$ for the number of outward points leaving a randomly chosen factor of the node, and $\widehat{G}_1^i$ for the number of points leaving a factor of the node by following a randomly chosen edge,

$$\hat{G}_0^i(y) = \hat{G}_0(1,y), \tag{9}$$

$$\hat{G}_1^i(y) = \frac{1}{m_i} \frac{\partial \hat{G}_0(x,y)}{\partial x}\bigg|_{x=1}. \tag{10}$$

In the same way, we can define the number of generating functions $\widehat{G}_0^o$ and $\widehat{G}_1^o$ for the number arriving at such a vertex,

$$\hat{G}_0^o(x) = \hat{G}_0(x,1), \tag{11}$$

$$\hat{G}_1^o(x) = \frac{1}{m_o} \frac{\partial \hat{G}_0(x,y)}{\partial y}\bigg|_{y=1}. \tag{12}$$

The average cardinality of the directed higher-order network,

$$\langle m \rangle = \sum_{m_i} \hat{P}(m_i, m_o) m_i = \sum_{m_o} \hat{P}(m_i, m_o) m_o. \tag{13}$$

With the idea of the factor graph, given the hyperdegree size k_i and k_o, and the hyperedge cardinality m_i and m_o, we can get four parameters to quantify the network. To simplify the network, we set $k = k_i = k_o$ and $m = m_i = m_o$. Given that the initial number of nodes in the network is N, we calculate the number of factor nodes in the network due to the relationship between k and m in the factor graph: $N_{factor} = N * k/m$. With the given parameters above, we can construct the directed random higher-order network conforming to the hyperdegree size k and the hyperedge cardinality m.

As shown in Fig. 1(a), we will have a model to generate the higher-order network divided into two steps. In the first step, a specific degree sequence was generated for the random network through the degree distribution function. The second step is through the method of random connections, combined with the introduction of the model previously defined by the concept of a random triangle, to generate the different directed random triangles and generate the directed higher-order network.[51]

In our directed higher-order network model, the network structure is random and sparse, so for a large enough network, it can be considered as a tree. That is, there is no circle in the network. The percolation problem of a directed higher-order network can be solved accurately by generating functions. To represent the initial degree distribution of a higher-order network, we define the hyperdegree distribution $P(k)$ and the hyperedge cardinality distribution $\hat{P}(m)$ correspond to the degree distributions of the nodes and factor nodes in the factor graph, respectively.[41]

As a random higher-order network map's component graph is a local tree, we take into account its corresponding factor graphs to depict percolation on directed higher-order networks. We can use a self-consistent equation to represent the probability of reaching a factor node belonging to the GCC from a node along with the edge,

$$\hat{S} = \sum_m \frac{m}{\langle m \rangle} \hat{P}(m) \left[1 - (1-S)^{m-1}\right]. \tag{14}$$

In Eq. (14), $m-1$ means that the factor node removes the edge from which it originates, $(1-S)^{m-1}$ represents the probability that a factor node cannot reach a node from the GCC; taking the sum and average over all the probabilities, we can get $\hat{S}$. In the same way, $(1-S)^{k-1}$ represents the probability that a normal node cannot reach a factor node from the GCC, S is the probability that a node from a node belongs to a GCC,

$$S = p\sum_k \frac{k}{\langle k\rangle}P(k)\left[1-\left(1-\hat{S}\right)^{k-1}\right]. \tag{15}$$

The order parameters of the percolation process, which are given by the probability R of finding a node in the GCC and the probability $\hat{R}$ of finding a hyperedge in the GCC,

$$R = 1-\sum_k P(k)\left(1-\hat{S}\right)^k, \tag{16}$$

$$\hat{R} = 1-\sum_m \hat{P}(m)(1-S)^m. \tag{17}$$

Equations (13)–(17) can be used to investigate the fundamental aspects of percolation and determine how robust higher-order networks are. In the directed higher-order networks, we consider the probability of finding a node in a GCC as the order parameter R to characterize the percolation problem. Through the definition of the giant in-component and the giant out-component, we give the formula of R_i and R_o,

$$R_i = p\left\{1-\sum_{k_ik_o} P_i(k_i,k_o)\left(1-\hat{s}\right)^i\right\}, \tag{18}$$

$$R_o = p\left\{1-\sum_{k_ik_o} P_o(k_i,k_o)\left(1-\hat{s}\right)^o\right\}. \tag{19}$$

Using the generating function $G_0(x,y)$, the above equation can be simplified as

$$R_i = p\left\{1-G_0\left(1-\hat{s}_i,1\right)\right\}, \tag{20}$$

$$R_o = p\left\{1-G_0\left(1,1-\hat{s}_o\right)\right\}. \tag{21}$$

Equations (17) and (19) give the relationship between the directed higher-order network R_i and S_i, R_o and S_o, but based on this formula, S or R cannot be solved. Therefore, we use Eq. (12) in Peng *et al.*,[42] to derive the following formula:

$$\hat{S} = 1-\hat{H}_1(1-S), \tag{22}$$

$$S = p\left(1-H_1\left(1-\hat{S}\right)\right). \tag{23}$$

The generating function in the undirected random higher-order network is represented by H in the formula.

Since directed higher-order networks can also be mapped to factor graphs, we give formulas for S and $\hat{S}$,

$$\hat{S}_i = \sum_{m_im_o}\frac{m}{\langle m\rangle}P(m_i,m_o)\left[1-\left(1-\hat{S}_i\right)^{m-1}\right], \tag{24}$$

$$S_i = p\sum_{k_ik_o}\frac{k}{\langle k\rangle}P(k_i,k_o)\left[1-\left(1-\hat{S}_i\right)^{k-1}\right]. \tag{25}$$

Similarly, we derive the formula for S_o and $\hat{S}_o$,

$$\hat{S}_o = \sum_{m_im_o}\frac{m}{\langle m\rangle}P(m_i,m_o)\left[1-\left(1-\hat{S}_i\right)^{m-1}\right], \tag{26}$$

$$S_o = p\sum_{k_ik_o}\frac{k}{\langle k\rangle}P(k_i,k_o)\left[1-\left(1-\hat{S}_i\right)^{k-1}\right]. \tag{27}$$

According to the above equation, the size of the giant in-component can be deduced by

$$\hat{S}_i = 1-\hat{G}_1^i\left(1,1-S_i\right), \tag{28}$$

$$S_i = p\left(1-G_1^i\left(1,1-\hat{S}_i\right)\right). \tag{29}$$

The giant out-component can be deduced by

$$\hat{S}_o = 1-\hat{G}_1^o\left(1-S_o,1\right), \tag{30}$$

$$S_o = p\left(1-G_1^o\left(1-\hat{S}_o,1\right)\right). \tag{31}$$

In Eq. (29), S_i represents the size of the GIN. The right end represents that if an edge of a node leads to the GIN, then this edge must belong to the GIN and has nothing to do with the in-degree. In the same way, in Eq. (31), S_o represents the size of the GOUT, and the right end of the formula represents a node. If there is an edge from the GOUT, then this edge must belong to the GOUT and has nothing to do with the out-degree.

With Eqs. (29)–(31), we compute the S_{GSCC} of Eq. (32) by bringing R_i and R_o into the network except for the GSCC size of the directed higher-order network,

$$S_{\mathrm{GSCC}} = p\left(1-G_1^o\left(1-\hat{S}_o,1\right)-G_1^i\left(1,1-\hat{S}_i\right)+G_1\left(1-\hat{S}_o,1-\hat{S}_i\right)\right). \tag{32}$$

In Eq. (32), S_{GSCC} represents the size of the strongly connected component of the network. The right side represents a node with an edge leading to the giant in-component, and an edge coming from the giant out-component. Then, it must reach all nodes in the GSCC, and all the GSCC nodes can reach this node. That is, it belongs to the GSCC, and the last term $G_1(1-\hat{S}_o,1-\hat{S}_i)$ represents the probability of compensating for repeated deductions of the first two terms. In this way, we can substitute Eqs. (2)–(6) to solve the GSCC of the directed higher-order network.

In studying the robustness of higher-order networks, we mainly focus on the size of the GSCC of the network. In addition, we also pay attention to the critical point when the network has phase transition, that is, when the node probability changes, calculate the size of the percolation threshold. In this paper, we calculate the percolation threshold of random directed higher-order networks and scale-free higher-order networks, which are consistent with Eq. (33),

$$p_c = \frac{\langle k\rangle}{\langle k(k-1)\rangle}\frac{\langle m\rangle}{\langle m(m-1)\rangle}, \tag{33}$$

where $\langle k\rangle$ represents the average degree of a directed higher-order network and $\langle m\rangle$ represents the average hyperedge cardinality of a directed higher-order network. From the formula of the percolation threshold, we can find that the percolation threshold of the directed higher-order network is only related to the network's k and m. When $\langle k\rangle$ and $\langle m\rangle$ are fixed, $\langle k(k-1)\rangle$ reveals the heterogeneity of the average degree of the network, $\langle m(m-1)\rangle$ reveals the heterogeneity of the hyperedge cardinality in the network. When k and m become larger and larger, the percolation threshold decreases gradually. We will discuss how to calculate percolation thresholds for different networks one by one in Sec. IV.

IV. EXPERIMENTAL RESULTS AND ANALYSIS

We used artificially constructed networks and real-world network datasets to study the robustness of the directed higher-order networks. We calculated the GCCs and percolation threshold through the theoretical formula to measure the robustness of the networks.

A. Homogeneous directed higher-order networks

As shown in Fig. 2, we perform Monte-Carlo simulations of the generated networks by constructing homogeneous directed higher-order networks. Different percolation experimental results are obtained by changing the network with different hyperdegree k and hyperedge cardinality m. It can be seen that the percolation threshold tends to decrease as the product of hyperdegree k and hyperedge cardinality m increases. The network's three GCCs undergo phase transitions simultaneously, and the sizes of the GIN and the GOUT are larger than the GSCC after the phase transition point.

The critical points of S_i and S_o of the directed higher-order network are the same as those of the tree random directed network and have nothing to do with the degree distribution and the correlation between the in-and out-degree. The GIN and the GOUT appear together with the GSCC, and it is impossible to emerge as one of them alone. Therefore, the critical points of the GIN and the GOUT of the homogeneous directed higher-order networks are the same, and the critical points of the GSCC are the same, which is confirmed by the simulation results.

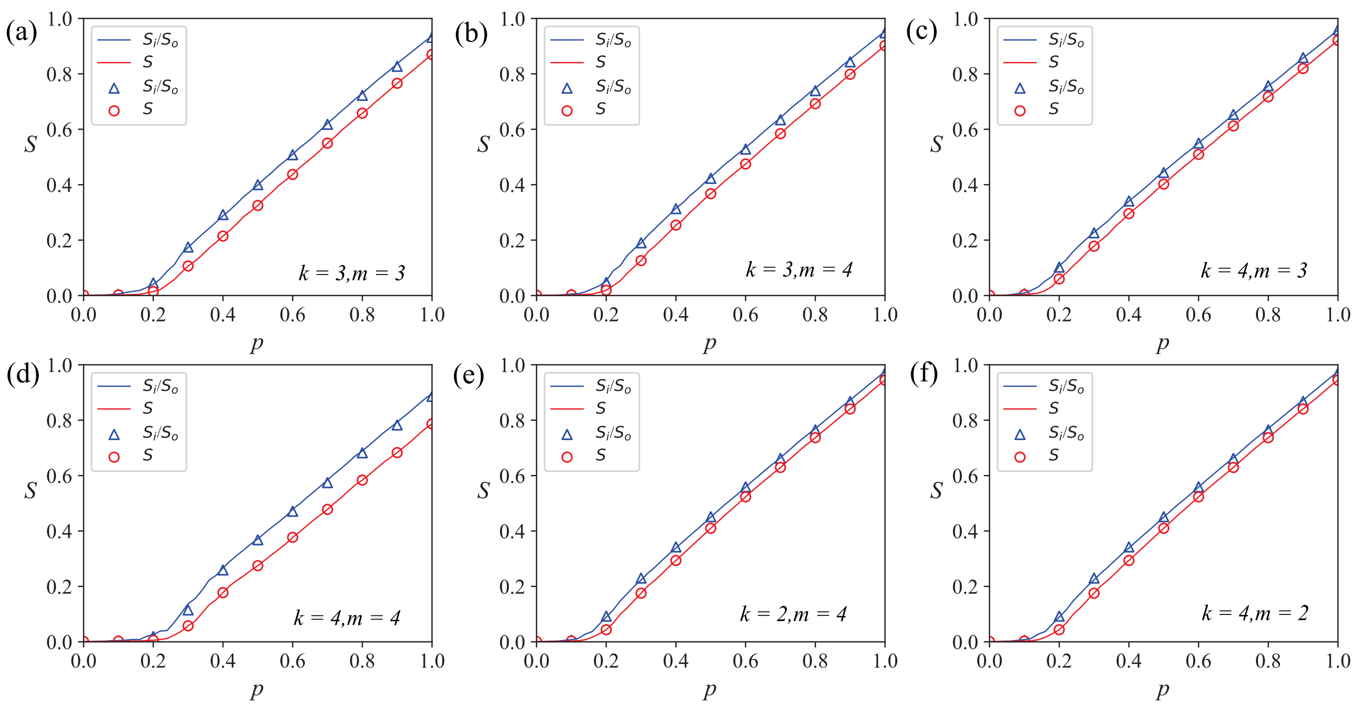

FIG. 2. Percolation on the homogeneous directed higher-order network. Experiment under different conditions: (a)–(f) $k \in \{2,3,4\}$, $m \in \{2,3,4\}$. With the increase of node removal probability $1-p$, the process of network disintegration is expressed by the size change of GCCs in the network. The percolation simulation of the directed higher-order network is consistent with the theory.

When the cardinality of the hyperdegree and hyperedge cardinality follows Poisson degree distribution, then

$$\frac{\langle k(k-1)\rangle}{\langle k\rangle}=\langle k\rangle, \tag{34}$$

$$\frac{\langle m(m-1)\rangle}{\langle m\rangle}=\langle m\rangle. \tag{35}$$

To simplify the model, we set the average hyperdegree is $\langle k\rangle=\langle k_i\rangle=\langle k_o\rangle$ and the average hyperedge cardinality $\langle m\rangle=\langle m_i\rangle=\langle m_o\rangle$. The average degree of the initial network is defined as k_{avg}, and $\langle k_{avg}\rangle$ can be represented by $\langle k\rangle$ and $\langle m\rangle$ of Eqs. (34) and (35),

$$\langle k_{\text{avg}}\rangle=\langle k\rangle\langle m\rangle. \tag{36}$$

Referring to the relation in Ref. 52, the percolation threshold of a directed random network can be deduced as

$$p_c=\frac{1}{\langle k_{\text{avg}}\rangle}. \tag{37}$$

After substituting the hyperdegree distribution and hyperedge cardinality, we get

$$p_c=\frac{\langle k\rangle}{\langle k(k-1)\rangle}\frac{\langle m\rangle}{\langle m(m-1)\rangle}. \tag{38}$$

In order to calculate the percolation threshold, Eqs. (20) and (21) are derived as follows:

$$F\left(R_i,S_i,p\right)=R_i-p\left\{1-G_0\left(1-\hat{s}_i,1\right)\right\}, \tag{39}$$

$$F\left(R_o,S_o,p\right)=R_o-p\left\{1-G_0\left(1,1-\hat{s}_o\right)\right\}. \tag{40}$$

Because we are picking the same in- and out-degree, including the hyperdegree and the hyperedge cardinality. Here, we only discuss the case of the in-degree of the directed random higher-order network, and the verification of the percolation threshold of the out-degree is similar to that of the in-degree. Putting the formula of $1-\hat{s}_i$ into Eq. (38), we get

$$F\left(R_i,S_i,p\right)=R_i-p\left\{1-G_0\left(\hat{G}_1^i\left(1-S_i,1\right),1\right)\right\}. \tag{41}$$

Through Eq. (41), the percolation threshold of the directed higher-order network can be solved, and the calculation curve in shown in Fig. 3. Insights that emphasize distinctive groupings and unique functional contributions of network nodes have received priority in the majority of network science discoveries. Importantly, the network of their interrelationships, generated by network edges, determines and expresses these functional contributions.[53] In order to better understand the importance of different hyperedges in a directed higher-order network, based on our directed higher-order

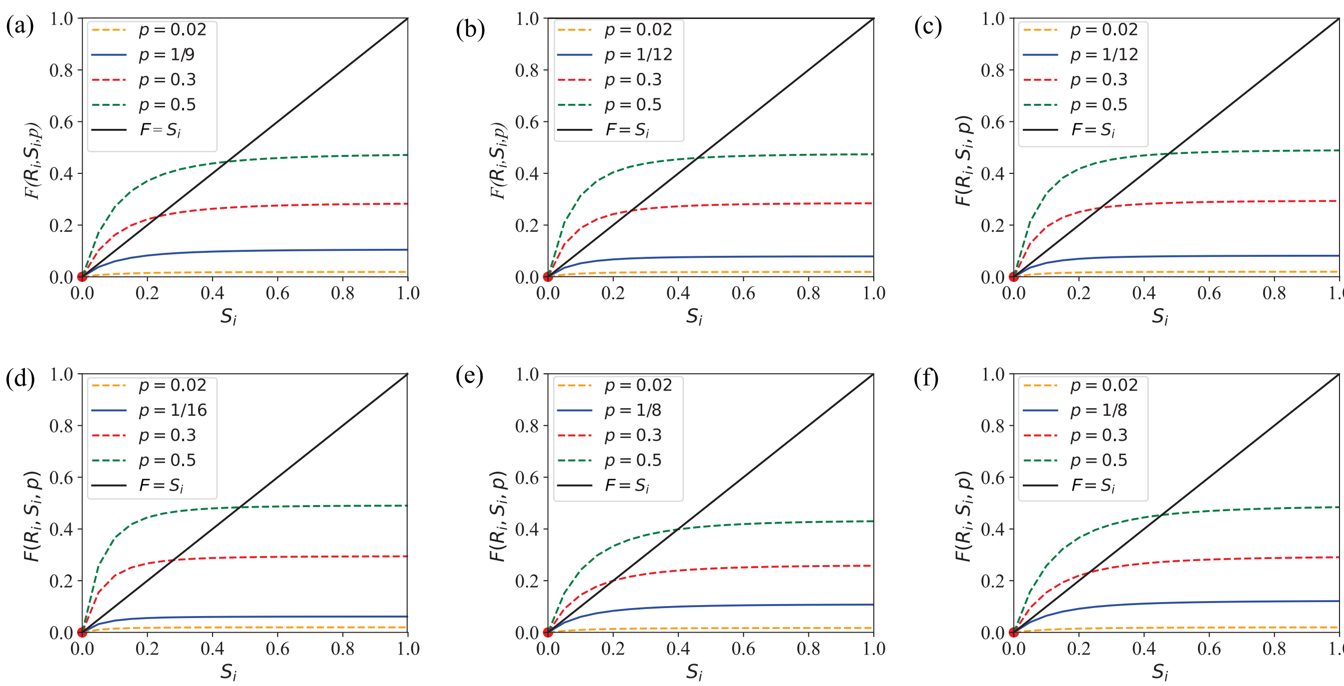

FIG. 3. Calculating the percolation threshold of the homogeneous directed higher-order network. The sizes of k and m for (a)–(f) correspond to those in Fig. 2. The black line in the figure is $F=S_i$. The curve $F(R_i,S_i,P)$ given by Eq. (40) is represented by different colors under different conditions, and the red intersection point represents the critical point of the percolation of the network. Obviously, the line is tangent to the curve F when the probability of preserving the node p is such that the numerator is equal to 1 and the denominator is equal to $k*m$.

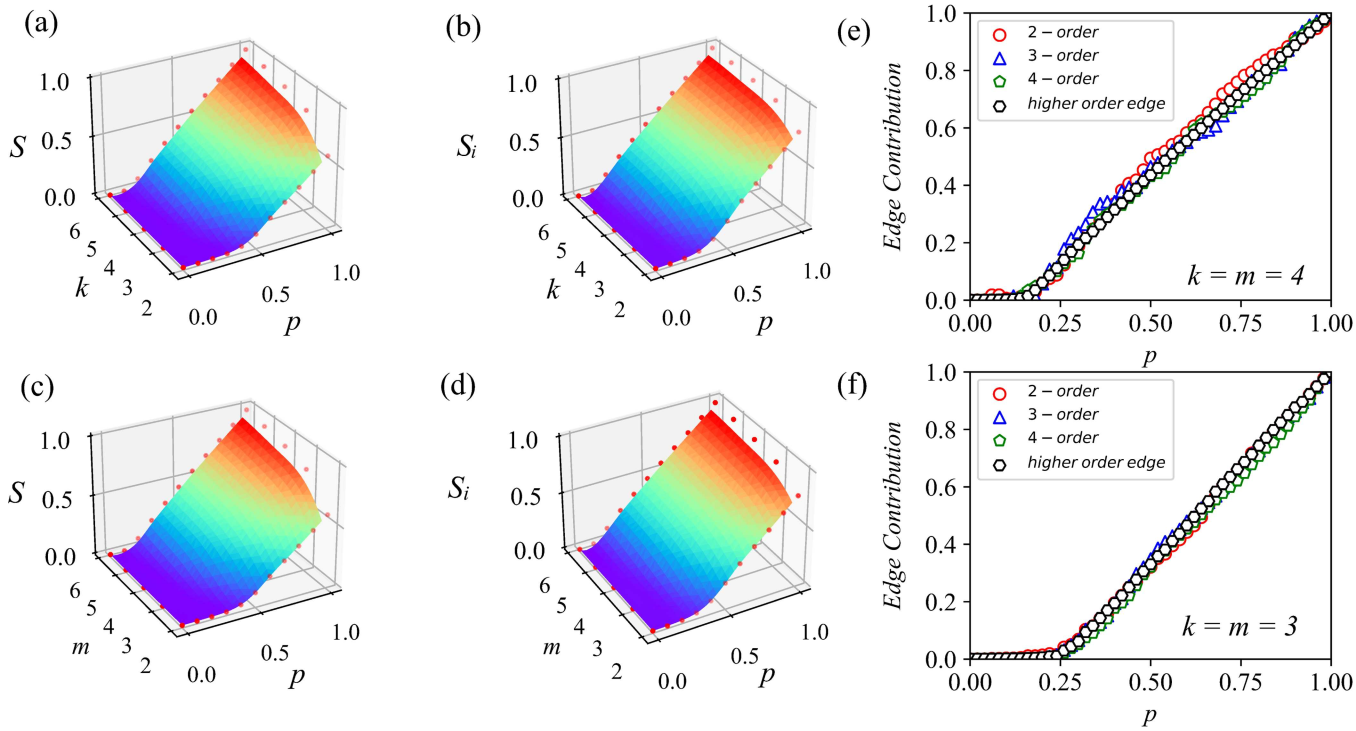

FIG. 4. The three-dimensional graph of the percolation of the homogeneous directed higher-order network and the proportion of edges of different orders in the percolation process of the network. (a)–(d) The three-dimensional graph corresponds to the percolation of the directed random higher-order network. The coordinates of the X axis represent the hyperedge cardinality m of the network and the size of the hyperdegree k, and k and m are taken as [2, 3, 4, 5, 6]. The Y axis represents the probability of retaining nodes in the network p, and the Z axis represents the probability of retaining nodes in the network S_i and S. Since S_i and S_o are equal in size, only S_i is shown here for brevity. (e) and (f) The contribution of higher-order edges and lower-order edges in the directed random higher-order network. The circle, triangle, pentagon, and hexagon in the graph, respectively, represent the size of hyperedges of different orders. The vertical axis represents the proportion of the number of edges of this order based on the size of the initial network.

network model, we study the contribution of each edge under relative initial GSCC. Without edges, a directed higher-order network would be a set of nodes without interaction.

In the experiment shown in Fig. 4, we counted the number of hyperedges of different orders in the strongly connected branches and expressed it by the contribution of edges, that is, the proportion of the number of hyperedges in the initial number of hyperedges in the percolation process. It can be seen from the experiment that the curve of edge contribution tends to be consistent with the curve of percolation in experiment part A. In the real network, we can use the experimental results to control the slump of the number of hyperedges.

Based on our simulation results, it can be seen that panels (c) and (f) in Fig. 4 represent the contribution of hyperedges in the directed higher-order network. In the simulation results, we find that the number of hyperedges is significantly larger than that of low-order edges and that higher-order interactions play a more vital part in the percolation of higher-order networks. In addition, we also calculate the number of hyperedges of different orders in GSCC, including 2-order edges, 3-order edges, and 4-order edges. When the node retention probability p is decreasing, and the removal probability $1 - p$ increases, the size of the network decreases gradually, and the number of hyperedges decreases continuously.

B. Heterogeneous directed higher-order networks

In addition to the homogeneous higher-order networks model that conforms to the Poisson degree distribution, we also construct heterogeneous directed higher-order networks that conform to the power-law degree distribution to represent the different higher-order interactions in complex networks.

First of all, we introduce in detail the construction method of a directed higher-order network conforming to a power-law distribution. By generating a directed scale-free directed network with a given in- and out-degree k_1,[51]

$$k_1 = 2m + 2k_2\left(1 - \frac{2m}{N}\right). \quad (42)$$

The degree distribution of the SF network follows the power-law distribution $P(k)$,

$$P(k) = \frac{(k+1)^{1-\lambda} - k^{1-\lambda}}{(k_M+1)^{1-\lambda} - k_m^{1-\lambda}} \tag{43}$$

k, k_M, and k_m are, respectively, the degree, maximum degree, and minimum degree of the network. For simplicity, we use a directed scale-free network with the same in- and out-degree. Then, we build our directed higher-order network model by adding a directed triangle conforming to the Poisson degree distribution k_2. p_t satisfies the following formula:

$$p_t = \frac{2k_2}{(N-1)(N-2)}. \tag{44}$$

Through the power-law distribution formula of Eq. (40), we give the formula of the directed higher-order network model conforming to the power-law distribution,

$$G_0(x,y) = \sum_{k_m}^{k_M} \frac{(k+1)^{1-\lambda} - k^{1-\lambda}}{\left(k_M+1\right)^{1-\lambda} - k_m^{1-\lambda}} x^{k_i} y^{k_o}. \tag{45}$$

The generating function of the hyperedge cardinality of a network,

$$\hat{G}_0(x,y) = \sum_{k_m}^{k_M} \frac{(k+1)^{1-\lambda} - k^{1-\lambda}}{\left(k_M+1\right)^{1-\lambda} - k_m^{1-\lambda}} x^{m_i} y^{m_o}. \tag{46}$$

For ease of calculation, we set the in-and out-hyperdegree of the network to be equal the in-and out-hyperedge cardinality. By Eqs. (40)–(42), we can construct directed random higher-order networks that conform to power-law distributions of particular k and m.

Combined with the definition of a random higher-order network and Eqs. (40)–(44), we can also calculate the percolation threshold of directed higher-order network in accordance with power-law distribution,

$$p_c = \frac{\langle k \rangle}{\langle k(k-1) \rangle} \frac{\langle m \rangle}{\langle m(m-1) \rangle}. \tag{47}$$

In the simulation experiment shown in Fig. 5, we found that based on SF network build directed higher-order network simulation and simulation is a certain distance, but the trend of each connected component of directed higher-order network and gives the theoretical solution of highly consistent, we by setting different k and m size, found that part of the simulation and the theoretical solution is the same.

In the complex network system, the phase transition and critical phenomena are for the infinite system, but the numerical simulation and the simulation experiment operate on the finite system. By setting the exponential coordinates of the Y axis and expanding the number of networks exponentially, we find that by 2 to the 13th power, the simulation results of the strongly connected branches of the directed higher-order networks of SF networks conform to the power-law distribution tend to the theoretical solution. Therefore,

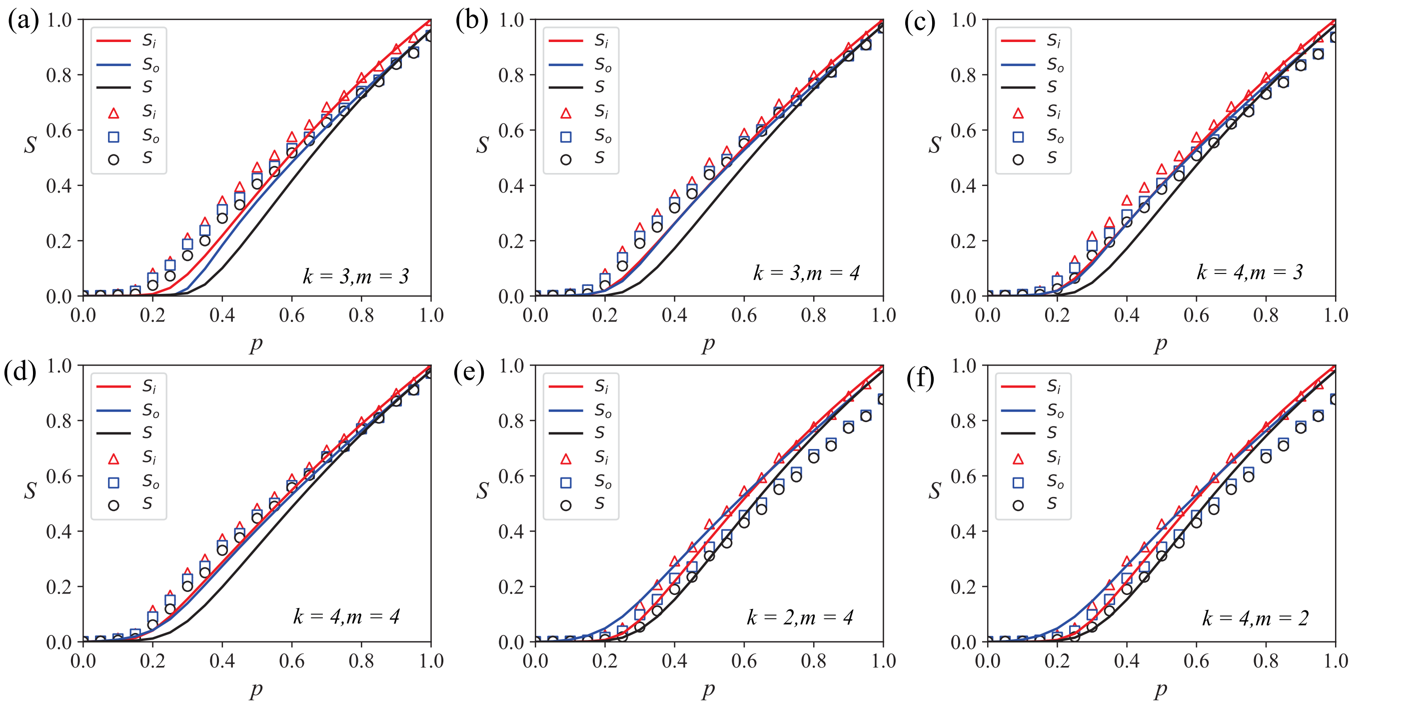

FIG. 5. Percolation on the heterogeneous directed SF higher-order network. Under different conditions: (a)–(f) $k \in \{2, 3, 4\}$, $m \in \{2, 3, 4\}$. The in- and out-hyperdegree and hyperedge cardinality power exponent λ to be 2.5. The percolation simulation of the directed higher-order network is consistent with the simulation.

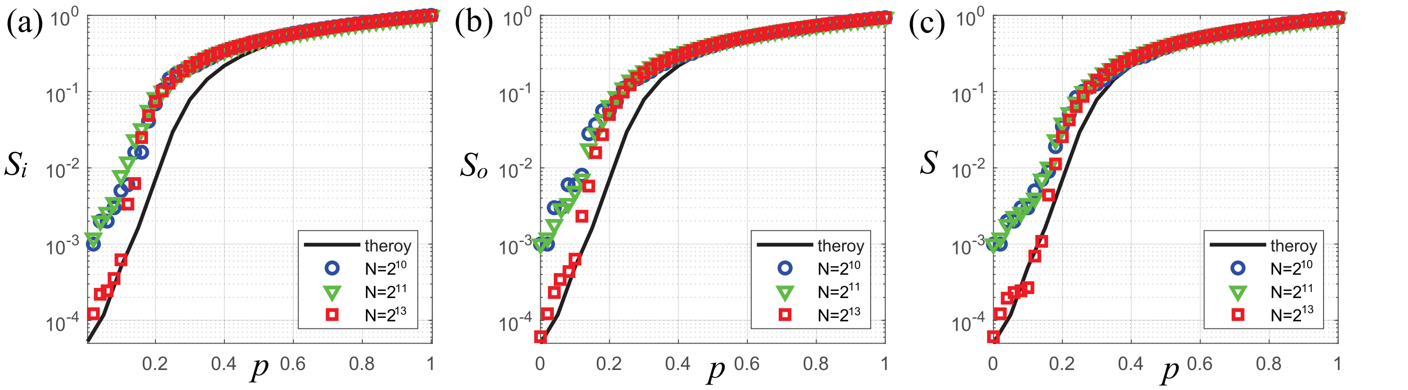

FIG. 6. The results of repeated experiments by modifying the scale of the network. The ordinate is different in connected components: (a) S_i, (b) S_o, and (c) S. In the experiment, as the network grows exponentially in size, the results of percolation simulation tend to be the theoretical solution. Compared with Fig. 5, coordinate log processing is performed on the vertical coordinate of the experiment to make it easier to find the experimental results.

through several experiments, the number of network nodes is changed by logarithmic growth. In addition, setting the network $k = m = 3$, we find that under the increasing number of network nodes, the percolation simulation results are more consistent with the theoretical solution in Fig. 6. In a first-order phase transition, the system transitions from one phase state to another at the phase transition point, and this transition occurs instantaneously. However, in the second-order phase transition, the intrinsic properties of the higher-order network show a trend of continuous change with the change of parameters, rather than sudden change. Therefore, from the process of percolation, we can find that the percolation phase transition of higher-order directed network is second-order phase transition.

C. Real-world directed higher-order networks

Directed networks are widely used in higher-order real networks, including social networks and biological networks. Here are two real network datasets applied in our experiment:[54]

Friendship networks (high school):[55] This dataset represents the directed network of reported possibilities. The node is a high school student. The authors used data collected at a high school in France, measured by parallel methods of face-to-face contact, wearable sensors, and contact diaries. A network of close contact between students is created using wearable sensors.

Neuronal networks:[29] This dataset calculates the topological properties of neuronal networks, such as degree distributions, synaptic multiplicity, and small-world properties. Nodes are different neurons. Using linear systems theory, the authors investigated how brain activity spreads in response to sensory or artificial stimuli and discovered a number of patterns of activity that might work as the behavioral substrates mentioned previously. Analyzed is the relationship between the chemical synaptic network and the gap junction.

To enhance the efficiency of the experiment, Table I's listing of seven parameters for the artificial network experiment. In each real-world dataset, face-to-face interactions were measured at a time resolution of 20 s. First, we create a weighted network based on the data, where the weights correspond to how many times a pair of nodes interacted across the total time range. Then, we remove any link with a weight less than a given threshold ζ and set the weight of the retained link to 1 to generate an unweighted network. The threshold ζ is a threshold to filter out certain connections with low interaction frequency. Finally, divide the data up into multiple time-windowed pieces and record all 2-hyperlinks or higher-order edges.

Specifically, if three nodes communicate with one another for a brief length of time, they are considered to form a three-body link. The frequency of 2-hyperlink in each segment is recorded. Through the generated directed higher-order network, we convert it into a factor graph and percolate the network of the factor graph to remove edges in the network. We count the number of higher-order edges in the network, including ordinary edges, 2-hyperlinks, and higher-order edges. We transform the hyperedges in the higher-order through Fig. 1(b) to obtain the real network with different sizes of hyperedges, as shown in Figs. 7(a) and 7(c).

TABLE I. The actual parameters in the real network, including the number of nodes N, the number of edges E, the average size of hyperdegree $\langle k\rangle$ and hyperedge cardinality $\langle m\rangle$, the maximum in- and out-hyperdegree k_{in}^{max} k_{out}^{max}, and the maximum hyperedge cardinality m_{max}. {$E1$, $E2$, $E3$, $E4$, $E5$} represents hyperedges of different sizes of the initial network.

Dataset	N	E	$\langle k\rangle$	$\langle m\rangle$	k_{in}^{max}	k_{out}^{max}	m_{max}	E1	E2	E3	E4	E5
Friendship	134	668	2.49	9.97	16	15	27	2008	15	26	29	14
C-elegans	279	2194	3.87	15.43	48	53	97	2010	48	44	75	73

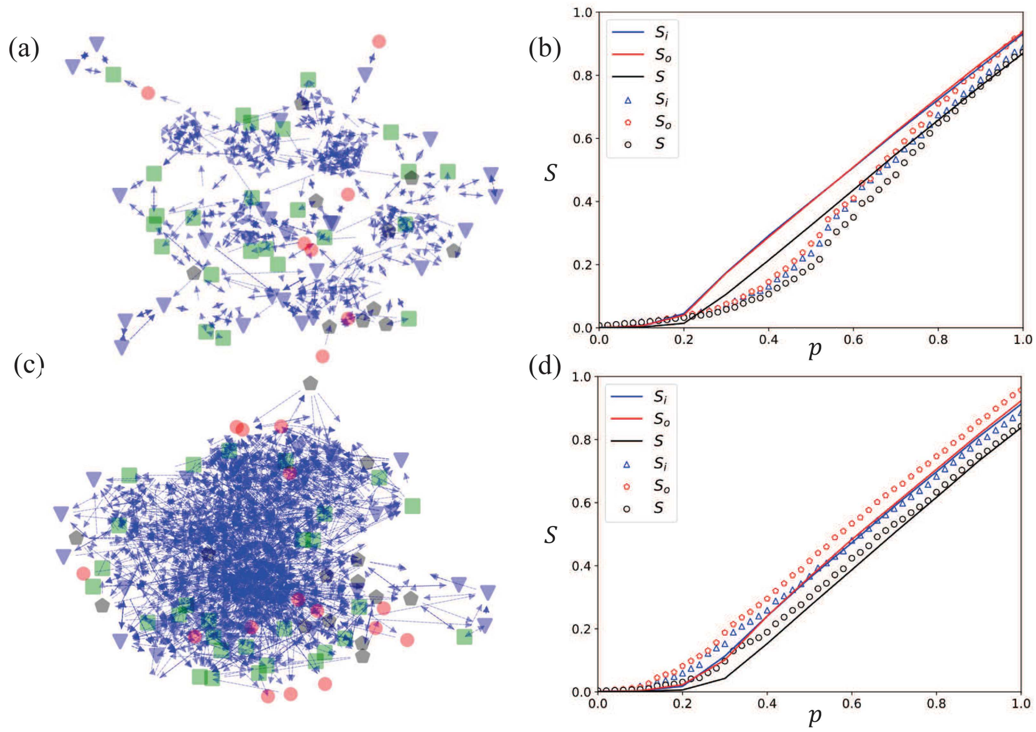

FIG. 7. Percolation on the social friendship networks and the biological neural networks. Panels (a) and (c) are factor graphs transformed from real networks, representing friendship networks and neuron networks, respectively. Blue lines in the figure represent edges in factor graphs, while triangles, squares, and pentagons represent hyperedges or factor nodes in factor graphs. Panels (b) and (d) in the figure is the percolation results and corresponding theoretical solutions. The corresponding theoretical parameters are shown in Table I, and the ordinate coordinates correspond to the GIN, GOUT, and GSCC sizes of the network, respectively.

With the decrease of the probability of retaining nodes in the factor graph, we find that the size of the GSCC in the real directed higher-order network gradually decreases, and a phase transition occurs at the percolation threshold point. As can be seen from Fig. 7, the percolation situation of our model on the real network is consistent with the theoretical solution. Similar phenomena are found in real-world networks as in model networks.

V. CONCLUSION

The significant contribution of this paper is that it has provided a theoretical framework of percolation for the study of higher-order networks. This framework has been used to study the robustness of homogeneous and heterogeneous directed higher-order networks. We have revealed the size variation of GIN, GOUT, and GSCC during percolation in a directed higher-order network and the size of the percolation threshold during the percolation phase transition. In addition, the network's percolation threshold has been calculated using the generating function and theoretical formulas, and the calculated results correspond to the Monte-Carlo simulation results.

In the experiment, we first constructed two different directed higher-order networks: homogeneous and heterogeneous directed higher-order networks and revealed the percolation process of the GIN, the GOUT, and the GSCC in the directed higher-order network by changing the network's hyperdegree k and hyperedge cardinality m. Increasing the hyperdegree distribution of heterogeneity or the hyperedge cardinality distribution of heterogeneity higher-order networks will make the network more vulnerable, weakening the higher-order network's robustness. Interestingly, in the homogeneous directed network, we calculated the sizes of the higher-order edges and low-order edges during the percolation process and found that their trends were consistent with the trend of percolation. Moreover, we showed the percolation process of the homogeneous directed higher-order network through the three-dimensional diagram. Finally, by visualizing social networks and biological neural networks in the real world, it is found that the simulated results correspond to the theoretical results again, further verifying our conclusions.

The results show that the robustness of directed higher-order networks at different scales can be effectively studied in our model. For example, when directed synaptic nodes in a network of biological neurons gradually fail, the above experimental results can explain how their function is affected, and the number of nodes that fail before the neural network breaks down. Our model captures the significant effects of multi-node interactions in the directed higher-order networks, and in future work, our model may be extended from spreading processes to other dynamical systems.

ACKNOWLEDGMENTS

This work was supported by the National Natural Science Foundation of China (NNSFC) (Grant Nos. 62072412, 61902359, 61702148, and 61672468), the Opening Project of Shanghai Key Laboratory of Integrated Administration Technologies for Information Security (Grant No. AGK2018001), the Program for Youth Innovation in Future Medicine, Chongqing Medical University (No. W0150), and the Natural Science Foundation of Chongqing (No. cstc2021jcyj-msxmX0132).

AUTHOR DECLARATIONS

Conflict of Interest

The authors have no conflicts to disclose.

Author Contributions

Dandan Zhao: Project administration (equal); Writing – original draft (lead); Writing – review & editing (equal). **Xianwen Ling:** Formal analysis (lead); Software (lead); Validation (lead). **Xiongtao Zhang:** Investigation (lead). **Hao Peng:** Conceptualization (equal); Funding acquisition (lead); Project administration (lead); Supervision (equal). **Ming Zhong:** Writing – original draft (lead). **Cheng Qian:** Writing – original draft (equal). **Wei Wang:** Conceptualization (lead); Funding acquisition (equal).

DATA AVAILABILITY

The data that support the findings of this study are openly available in sociopatterns at http://www.sociopatterns.org, Ref. 54.

REFERENCES

[1] M. E. Newman, *Networks: An Introduction* (Oxford University Press, 2010).
[2] M. E. Newman, "The structure and function of networks," Comput. Phys. Commun. **147**, 40–45 (2002).
[3] A. Zhu, "Personalised recommendation algorithm for social network based on two-dimensional correlation," Int. J. Auton. Adapt. Commun. Syst. **13**, 195–209 (2020).
[4] P. Bartesaghi, G. P. Clemente, and R. Grassi, "Taxonomy of cohesion coefficients for weighted and directed multilayer networks," Chaos Soliton. Fract. **166**, 112968 (2023).
[5] M. Morrison and L.-S. Young, "Chaotic heteroclinic networks as models of switching behavior in biological systems," Chaos **32**, 123102 (2022).
[6] E. Saucan, R. Sreejith, R. Vivek-Ananth, J. Jost, and A. Samal, "Discrete Ricci curvatures for directed networks," Chaos Soliton. Fract. **118**, 347–360 (2019).
[7] M. E. Newman, S. Forrest, and J. Balthrop, "Email networks and the spread of computer viruses," Phys. Rev. E **66**, 035101 (2002).
[8] R. Cohen, K. Erez, D. Ben-Avraham, and S. Havlin, "Resilience of the internet to random breakdowns," Phys. Rev. Lett. **85**, 4626 (2000).
[9] X. Huang, J. Gao, S. V. Buldyrev, S. Havlin, and H. E. Stanley, "Robustness of interdependent networks under targeted attack," Phys. Rev. E **83**, 065101 (2011).
[10] J. Gao, S. V. Buldyrev, H. E. Stanley, and S. Havlin, "Networks formed from interdependent networks," Nat. Phys. **8**, 40–48 (2012).
[11] Q. Chen and R. A. Bridges, "Automated behavioral analysis of malware: A case study of WannaCry ransomware," in *2017 16th IEEE International Conference on Machine Learning and Applications (ICMLA)* (IEEE, 2017), pp. 454–460.
[12] P. Yu, R. Xu, M. J. Abramson, S. Li, and Y. Guo, "Bushfires in Australia: A serious health emergency under climate change," Lancet Planet. Health **4**, e7–e8 (2020).
[13] Y.-K. Wu, Y.-C. Chen, H.-L. Chang, and J.-S. Hong, "The effect of decision analysis on power system resilience and economic value during a severe weather event," IEEE Trans. Ind. Appl. **58**, 1685–1695 (2022).
[14] S. Boccaletti, V. Latora, Y. Moreno, M. Chavez, and D.-U. Hwang, "Complex networks: Structure and dynamics," Phys. Rep. **424**, 175–308 (2006).
[15] M. Li, R.-R. Liu, L. Lü, M.-B. Hu, S. Xu, and Y.-C. Zhang, "Percolation on complex networks: Theory and application," Phys. Rep. **907**, 1–68 (2021).
[16] D. S. Callaway, M. E. Newman, S. H. Strogatz, and D. J. Watts, "Network robustness and fragility: Percolation on random graphs," Phys. Rev. Lett. **85**, 5468 (2000).
[17] M. Boguñá and M. Á. Serrano, "Generalized percolation in random directed networks," Phys. Rev. E **72**, 016106 (2005).
[18] N. Schwartz, R. Cohen, D. Ben-Avraham, A.-L. Barabási, and S. Havlin, "Percolation in directed scale-free networks," Phys. Rev. E **66**, 015104 (2002).
[19] F. Battiston, G. Cencetti, I. Iacopini, V. Latora, M. Lucas, A. Patania, J.-G. Young, and G. Petri, "Networks beyond pairwise interactions: Structure and dynamics," Phys. Rep. **874**, 1–92 (2020).
[20] Z.-K. Zhang and C. Liu, "A hypergraph model of social tagging networks," J. Stat. Mech.: Theory Exp. **2010**, P10005 (2010).
[21] F. Hu, L. Ma, X.-X. Zhan, Y. Zhou, C. Liu, H. Zhao, and Z.-K. Zhang, "The aging effect in evolving scientific citation networks," Scientometrics **126**, 4297–4309 (2021).
[22] G. Bianconi, *Higher-Order Networks* (Cambridge University Press, 2021).
[23] G. St-Onge, V. Thibeault, A. Allard, L. J. Dubé, and L. Hébert-Dufresne, "Master equation analysis of mesoscopic localization in contagion dynamics on higher-order networks," Phys. Rev. E **103**, 032301 (2021).
[24] M. Xie, X.-X. Zhan, C. Liu, and Z.-K. Zhang, "An efficient adaptive degree-based heuristic algorithm for influence maximization in hypergraphs," Inf. Process. Manage. **60**, 103161 (2023).
[25] A. Arenas, A. Díaz-Guilera, J. Kurths, Y. Moreno, and C. Zhou, "Synchronization in complex networks," Phys. Rep. **469**, 93–153 (2008).
[26] U. Alvarez-Rodriguez, F. Battiston, G. F. de Arruda, Y. Moreno, M. Perc, and V. Latora, "Evolutionary dynamics of higher-order interactions in social networks," Nat. Hum. Behav. **5**, 586–595 (2021).
[27] Y. Nie, X. Zhong, T. Wu, Y. Liu, T. Lin, and W. Wang, "Effects of network temporality on coevolution spread epidemics in higher-order network," J. King Saud Univ.-Comput. Inf. Sci. **34**(6), 2871–2882 (2022).
[28] U. Alvarez-Rodriguez, F. Battiston, G. Ferraz de Arruda, Y. Moreno, M. Perc, and V. Latora, "Collective games on hypergraphs," in *Higher-Order Systems* (Springer, 2022), pp. 377–388.
[29] L. R. Varshney, B. L. Chen, E. Paniagua, D. H. Hall, and D. B. Chklovskii, "Structural properties of the Caenorhabditis elegans neuronal network," PLoS Comput. Biol. **7**, e1001066 (2011).
[30] E. Vasilyeva, A. Kozlov, K. Alfaro-Bittner, D. Musatov, A. Raigorodskii, M. Perc, and S. Boccaletti, "Multilayer representation of collaboration networks with higher-order interactions," Sci. Rep. **11**, 1–11 (2021).
[31] Y. Tang, D. Shi, and L. Lü, "Optimizing higher-order network topology for synchronization of coupled phase oscillators," Commun. Phys. **5**, 1–12 (2022).
[32] M. Teteryatnikova, "Systemic risk in banking networks: Advantages of "tiered" banking systems," J. Econ. Dyn. Control **47**, 186–210 (2014).
[33] J.-H. Zhao, H.-J. Zhou, and Y.-Y. Liu, "Inducing effect on the percolation transition in complex networks," Nat. Commun. **4**, 1–6 (2013).
[34] D. Stauffer and A. Aharony, *Introduction to Percolation Theory* (Taylor & Francis, 2018).
[35] Z. Wang, D. Zhou, and Y. Hu, "Group percolation in interdependent networks," Phys. Rev. E **97**, 032306 (2018).
[36] S. N. Dorogovtsev, J. F. F. Mendes, and A. N. Samukhin, "Giant strongly connected component of directed networks," Phys. Rev. E **64**, 025101 (2001).
[37] M. A. Serrano and P. De Los Rios, "Interfaces and the edge percolation map of random directed networks," Phys. Rev. E **76**, 056121 (2007).
[38] P. van der Hoorn and N. Litvak, "Phase transitions for scaling of structural correlations in directed networks," Phys. Rev. E **92**, 022803 (2015).
[39] A. Bretto, "Hypergraph theory: An introduction," in *Mathematical Engineering* (Springer, Cham, 2013).
[40] X. Xie, X. Zhan, Z. Zhang, and C. Liu, "Vital node identification in hypergraphs via gravity model," Chaos **33**, 013104 (2023).

[41] H. Sun and G. Bianconi, "Higher-order percolation processes on multiplex hypergraphs," Phys. Rev. E **104**, 034306 (2021).
[42] H. Peng, C. Qian, D. Zhao, M. Zhong, J. Han, and W. Wang, "Targeting attack hypergraph networks," Chaos **32**, 073121 (2022).
[43] H. Peng, C. Qian, D. Zhao, M. Zhong, X. Ling, and W. Wang, "Disintegrate hypergraph networks by attacking hyperedge," J. King Saud Univ.-Comput. Inf. Sci. **34**(7), 4679–4685 (2022).
[44] D. Zhao, R. Li, H. Peng, M. Zhong, and W. Wang, "Higher-order percolation in simplicial complexes," Chaos Soliton. Fract. **155**, 111701 (2022).
[45] D. Zhao, R. Li, H. Peng, M. Zhong, and W. Wang, "Percolation on simplicial complexes," Appl. Math. Comput. **431**, 127330 (2022).
[46] J.-H. Kim and K.-I. Goh, "Higher-order components in hypergraphs," arXiv:2208.05718 (2022).
[47] O. T. Courtney and G. Bianconi, "Dense power-law networks and simplicial complexes," Phys. Rev. E **97**, 052303 (2018).
[48] A. Ducournau and A. Bretto, "Random walks in directed hypergraphs and application to semi-supervised image segmentation," Comput. Vis. Image Underst. **120**, 91–102 (2014).
[49] X. Liu, L. Pan, H. E. Stanley, and J. Gao, "Controllability of giant connected components in a directed network," Phys. Rev. E **95**, 042318 (2017).
[50] E. Kenah and J. M. Robins, "Second look at the spread of epidemics on networks," Phys. Rev. E **76**, 036113 (2007).
[51] H. Wang, C. Ma, H.-S. Chen, Y.-C. Lai, and H.-F. Zhang, "Full reconstruction of simplicial complexes from binary contagion and Ising data," Nat. Commun. **13**, 1–10 (2022).
[52] J. Shao, S. V. Buldyrev, L. A. Braunstein, S. Havlin, and H. E. Stanley, "Structure of shells in complex networks," Phys. Rev. E **80**, 036105 (2009).
[53] J. Faskowitz, R. F. Betzel, and O. Sporns, "Edges in brain networks: Contributions to models of structure and function," Netw. Neurosci. **6**, 1–28 (2022).
[54] See http://www.sociopatterns.org for information about "Sociopatterns collaboration" (2021).
[55] R. Mastrandrea, J. Fournet, and A. Barrat, "Contact patterns in a high school: A comparison between data collected using wearable sensors, contact diaries and friendship surveys," PLoS One **10**, e0136497 (2015).